Proceedings of OMAE2009
28th International Conference on Ocean, Offshore and Arctic Engineering
31. mai – 5. june 2009, Honolulu, Hawaii

OMAE2009-79389

SYSTEMATIC INVESTIGATION OF LOADS AND MOTIONS OF A BULK CARRIER IN EXTREME SEAS

Günther F. Clauss
Ocean Engineering Division
Institute of Land and Sea Transportation
Technical University of Berlin
Germany
Email: clauss@naoe.tu-berlin.de

André Kauffeldt*
Ocean Engineering Division
Institute of Land and Sea Transportation
Technical University of Berlin
Germany
Email: Kauffeldt@naoe.tu-berlin.de

Marco Klein
Ocean Engineering Division
Institute of Land and Sea Transportation
Technical University of Berlin
Germany
Email: Klein@naoe.tu-berlin.de

ABSTRACT

During their lifetime ships often operate in severe weather and rough sea states. To ensure survival, a precise knowledge of global and local loads is an inevitable integral part for a safe design. One of the key parameters for ship design is the vertical bending moment. Not only vertical forces but also longitudinal forces can contribute to this bending moment. As the overall effect of longitudinal forces is still not fully understood, all structural loads are investigated in detail, especially in extreme seas.

Within the project "Handling Waves", funded by the European Union, three segmented ships, equipped with force transducers, are investigated systematically at several cruising speeds and in various deterministic wave sequences to identify structural loads, i.e. the vertical bending moment as well as the superimposing longitudinal forces.

Within this paper a detailed overview of the results for the bulk carrier is given and both, frequency- and time-domain results are presented. With Response Amplitude Operators (RAOs), delivered by frequency-domain analysis, the profound data for the standard assessment of structures, concerning seakeeping behaviour, operational limitations and fatigue are obtained. In addition, time domain analyses in rogue waves such as the so called "New Year Wave" provide essential data for extreme motions and structural loads.

Former investigations on a FPSO revealed that, due to the location of the neutral axis, the longitudinal forces are significant and generate a counteracting moment compared to the vertical bending moment [1]. The new results show to what extent the above mentioned conclusions are applicable for various hull designs.

INTRODUCTION

Ship losses such as the sinking of the mono-hull tankers Erika (1999) and Prestige (2002, Fig. 1) as well as of the double-hull tanker Ievoli Sun (2000, Fig. 2) illustrate that structural failures in heavy seas are still a major problem.

A key issue is the vertical bending moment. According to the IACS-Common Rules [2] the classification societies are considering a ship in design waves, and distinguish between hogging and sagging condition. The associated vertical wave bending moments provide a basis for dimensioning the ship's hull. Longitudinal forces are considered to be small. Thus, they are neglected for design tasks. According to former investigations [1], however, the longitudinal forces may affect the loads on the ship's hull significantly.

To determine the effect of the longitudinal forces on various ship types a sophisticated approach is required considering the investigation of ship responses in irregular seas. So far four different ship types, i.e. a FPSO, a Ro/Ro vessel, a container feeder and a bulk carrier, have been analysed in head seas and in following seas at different cruising speeds. This paper focuses on

* Address all correspondence to this author

Fig. 1: Prestige sinking (source: dpa)

Fig. 2: Ievoli Sun sinking (source: dpa)

experimental and numerical analyses of the bulk carrier, and presents results in frequency and time domain. In particular, ship loads in tailored rogue waves are studied.

EXPERIMENTAL SETUP

The model tests are conducted in the seakeeping basin of the Ocean Engineering Division, Technical University Berlin (TUB), at model scale 1:70. The seakeeping basin with an overall length of 110 m and an effective measuring section of about 90 m offers a width of 8 m at a water depth of up to 1.1 m. A computer controlled, electrical driven wave generator is installed. Due to a special hinged, segmented wave board the unit can be used both as flap type and piston type wave maker. The software of the control unit allows the generation of transient wave packages, deterministic irregular sea states with predefined characteristics as well as tailor-made critical wave sequences [3].

The underlying wave model is based on the superposition of wave components taking into account the non-linear interaction between high-order wave components [4]. This technique has been established to reproduce a large variety of wave sequences such as single freak waves as well as groups of rogue waves embedded in irregular sea states in order to investigate the response of floating structures to an extreme, but realistic, wave environment [5], [6].

The experiments are carried out with a wooden model of the bulk carrier subdivided at $L_{PP}/2$. The main dimensions of the bulk carrier are:

- Length overall L_{oa} = 186.45 m
- Length between perpendiculars L_{pp} = 177.00 m
- Breadth moulded B = 30.00 m
- Depth moulded D = 16.20 m
- Draught T = 11.80 m
- Displacement Δ = 52556 t

The two segments of the model are connected by three force transducers: Two of them are arranged close to the deck level and the third one is installed underneath the bottom of the model (Fig. 3). The force transducers register the occurring longitudinal forces during the model test. These data in combination with the known geometrical arrangement of the force transducers allow the analysis of the dynamic distribution of forces and moments at the midship section (Fig. 4). Based on these informations the resulting dynamic neutral axis, the vertical bending moment and axial forces are obtained. It should be noted that in this case the neutral axis is based on the dynamic pressure forces – contributions from hydrostatic pressure as well as the centre of area of structural components are not considered.

During the tests the model is towed using a triangular towing arrangement with a spring in front and a counter weight behind the model pulling the model without influencing the pitch and surge motions.

The ship motions are recorded by an optical tracking system with four infrared cameras covering an area of 10 by 7 meters. The cameras are installed on a special

Fig. 3: Model of the segmented bulk carrier at model scale 1:70

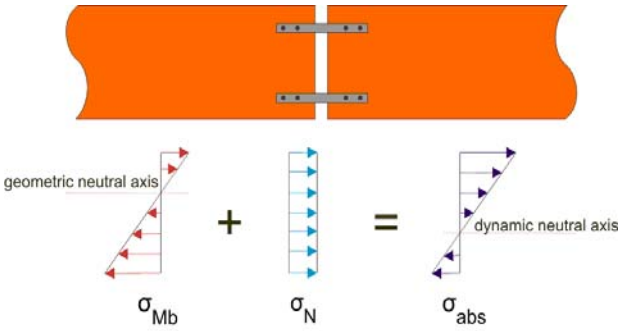

Fig. 4: The absolute stress distribution σ_{abs} results from the superposition of the bending stress σ_{Mb} and the axial stress σ_N.

carriage traveling on roof-mounted rails at the same forward speed as the ship model. The system enables high precision, contact-free motion tracking over large distances by following the trajectories of infrared light emitting diodes mounted on the ship model.

EXPERIMENTAL PROGRAM

The experimental program includes investigations in frequency and time domain. In frequency domain the aim of the model tests is the determination of the response in terms of transfer functions for each particular physical value. Thus, with frequency-domain analysis the profound data for the standard assessment of structures, concerning seakeeping behaviour, operational limitations and fatigue are obtained. The transient wave package technique is applied, which is a powerful and efficient tool for the fast determination of the response amplitude operators (RAOs) [7].

Time-domain analysis in real rogue waves gives indispensable data on extremes, i.e. motions and structural forces. For this purpose the ship is investigated at stationary conditions as well as at different forward speeds for both head and following seas.

One of the model wave sequences is the well-known "New Year Wave" (NYW). This wave has been recorded during a storm on January 1, 1995 at the Draupner platform in the North Sea [8]. A giant single wave (H_{max} = 25.63 m) with a crest height of ζ_c = 18.5 m occurred in a surrounding sea state characterised by a significant wave height of H_s =11.92 m (H_{max}/H_s = 2.15). The water depth at the location is d = 70 m. Fig. 5 illustrates a comparison of the New Year Wave simulated at the sea keeping basin (scale 1:70) compared to the original wave sequence measured at the Draupner platform.

FREQUENCY DOMAIN RESULTS

As mentioned before the frequency domain results provide a basis to define the character of the ship regarding the sea keeping behaviour. The model tests are used to validate the numerical results which are obtained by the diffraction / radiation program system WAMIT.

WAMIT

For the evaluation of motions, forces and bending moments the program system WAMIT (Wave Analysis, developed at Massachusetts Institute of Technology) for wave/structure interaction at zero-speed [9] is applied.

Hydrodynamic analysis

The analysis of a compact rigid body with six degrees of freedom is described by a boundary value problem. The total velocity potential $\phi(\underline{x},t)$ for an inviscid, incompressible fluid and irrotational flow follows from Laplace equation

$$\Delta\phi(\underline{x},t) = 0. \qquad (1)$$

Assuming linear theory the total velocity potential ϕ is given as superposition of the individual potentials due to incoming plane waves as well as the wave systems arising from diffraction (φ_7) and the motions of the body ($\varphi_{1...6}$)

$$\phi(\underline{x},t) = \phi_0 + \phi_7 + \sum_{k=1}^{6} \phi_k \qquad (2)$$

with ϕ_0 incident wave potential

ϕ_7 potential of scattered wave field (diffraction)

ϕ_k potential of the radiation wave field evoked by a motion in mode k.

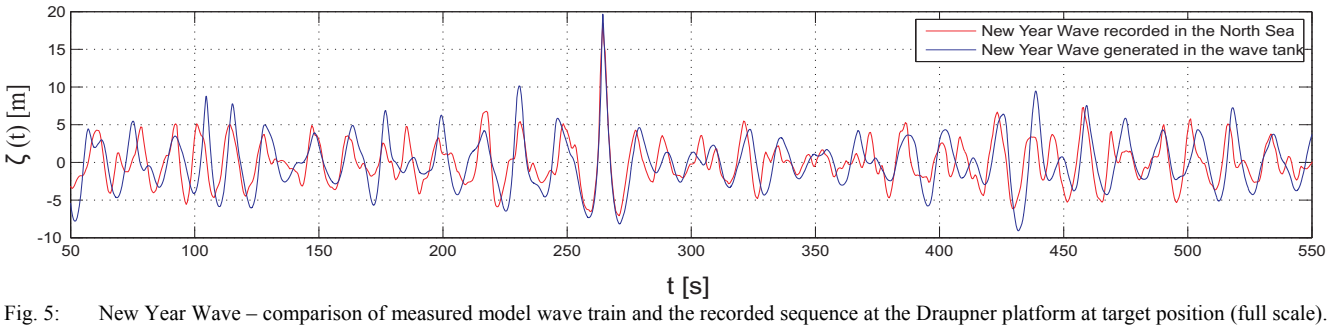

Fig. 5: New Year Wave – comparison of measured model wave train and the recorded sequence at the Draupner platform at target position (full scale).

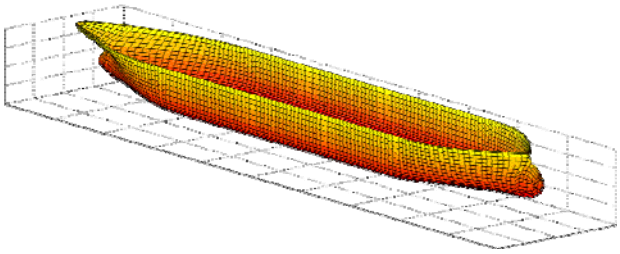

Fig. 6: WAMIT-mesh of the bulk carrier

On the wetted body surface normal velocity is zero. For an oscillating body this condition results into:

$$\frac{\partial \phi_i}{\partial n} = \underline{\dot{s}} \cdot \underline{n}^*, \quad on\ S_b\ . \tag{3}$$

The linearized kinematic and dynamic boundary conditions on the free surface are merged into the generalized free surface condition:

$$\frac{\partial \phi_i}{\partial z} - \frac{\omega^2}{g}\phi_i = 0\ . \tag{4}$$

On the ocean bottom normal velocities are zero:

$$\frac{\partial \phi_i}{\partial n} = 0, \quad for\ z = -d\ . \tag{5}$$

ϕ_i *(i=0,1,...,7)* holds for any potential, which are superimposed to form the complete solution. Finally in the far field the Sommerfeld radiation condition for the scatter and radiation wave field must be satisfied:

$$\lim_{R\to\infty} \sqrt{R}\left(\frac{\partial \phi_j}{\partial R} - ik\phi_j\right) = 0, \quad j = 1,...,7\ . \tag{6}$$

The initial boundary value problem, defined by Laplace equation (1) and the above boundary conditions, is transformed into integral equations by applying Green's second theorem [10] and, after some manipulation, we obtain:

$$\begin{aligned} &2\pi\phi + \iint_{S_b}\left(\phi\, G_n^{(0)} - G^{(0)}\phi_n\right)dS \\ &+ \int_{-\infty}^{t}\iint_{S_b}\left(\phi\, G_{tn} - G_t\phi_n\right)dS\ d\tau = 0. \end{aligned} \tag{7}$$

This equation allows solving for the unknown scatter and radiation potentials on the mean position of the body surface S_b in time-domain. In frequency-domain the second integral term vanishes to zero. The wetted body surface has to be discretized into *N* panels (Fig. 6) where the boundary conditions are satisfied on the respective collocation points. Based on this potential the instationary Bernoulli equation gives the (linearized) dynamic pressure:

$$p_{dyn} = -\rho\frac{\partial \phi}{\partial t} \tag{8}$$

which defines the forces and moments acting on the body:

$$\underline{F} = \iint_{S_b} p_{dyn}\,\underline{n}^*\,dS\ . \tag{9}$$

With Newton's second law, and assuming the body and its forcing comprise a stable linear system, the equation of motion is obtained [11]:

$$(M+a)\ddot{\underline{s}} + B\dot{\underline{s}} + C\underline{s} + \int_{-\infty}^{t} K(t-\tau)\dot{\underline{s}}(\tau)d\tau = F(t)\ . \tag{10}$$

In frequency-domain, Eq. (10) is solved for harmonic excitation. Divided by the wave amplitude ζ_a the equation is reduced to:

$$(-\omega^2(M+a) - i\omega B + C)H(\omega) = \frac{\underline{F}_a}{\zeta_a}e^{i\gamma} \tag{11}$$

with the response amplitude operator $H(\omega)=\underline{s}_a/\zeta_a e^{i\varepsilon}$, representing amplitude $\underline{s}_a$ and phase shift ε of the motion in frequency-domain. γ is the phase of forcing.

Hydroelastic analysis

The program WAMIT allows the analysis of generalized modes of flexural motions, in addition to the usual six degrees of rigid-body motions. By defining the ship bending modes the associated structural deformations can be calculated. Legendre polynomials $P_i(x)$, $i = 2, 3,\ldots$ [12] are found to approximate well the bending modes of a ship [13]. The deflection line for each bending mode is given by the product of the calculated amplitude and the corresponding Legendre polynomial.

$$w_i(x) = s_{ia}\cdot P_{i-5}(x), \quad i = 7,8,... \tag{12}$$

The indexing takes into account, that the first 6 indices are reserved for the conventional rigid body motions. For several bending modes, the total deflection results from complex addition of the individual deflection lines. Twice differentiation of the deflection line, multiplied with the flexural stiffness results in the bending moment of the ship:

$$M_b(x) = -w''(x)\cdot EI_y(x) \tag{13}$$

The above WAMIT procedure has been successfully used to analyze vertical bending moments of stationary ships with high block coefficient [14].

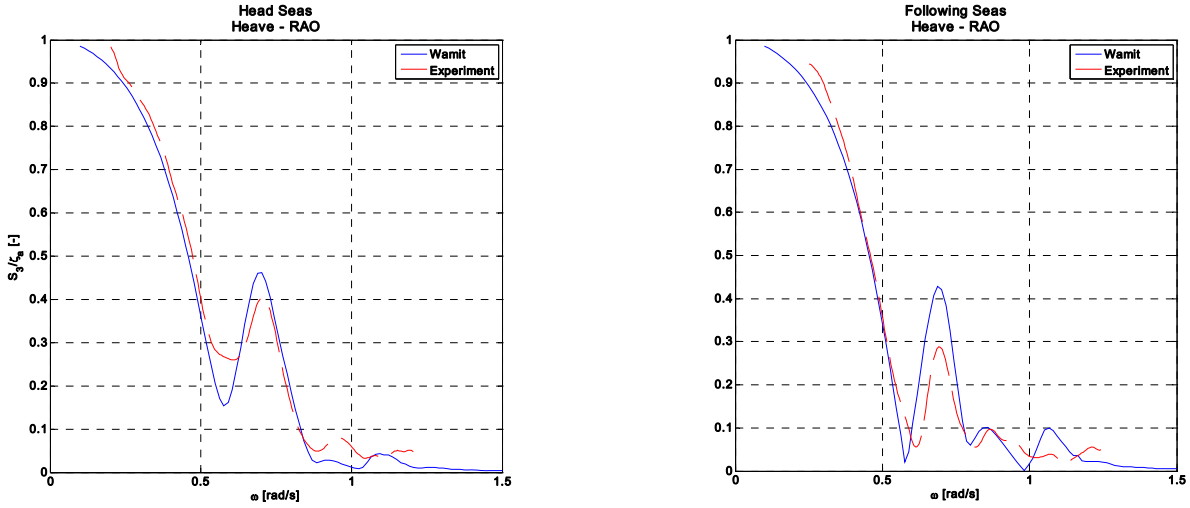

Fig. 7: Comparison of measured and calculated Response Amplitude Operators (RAO) for the heave motion

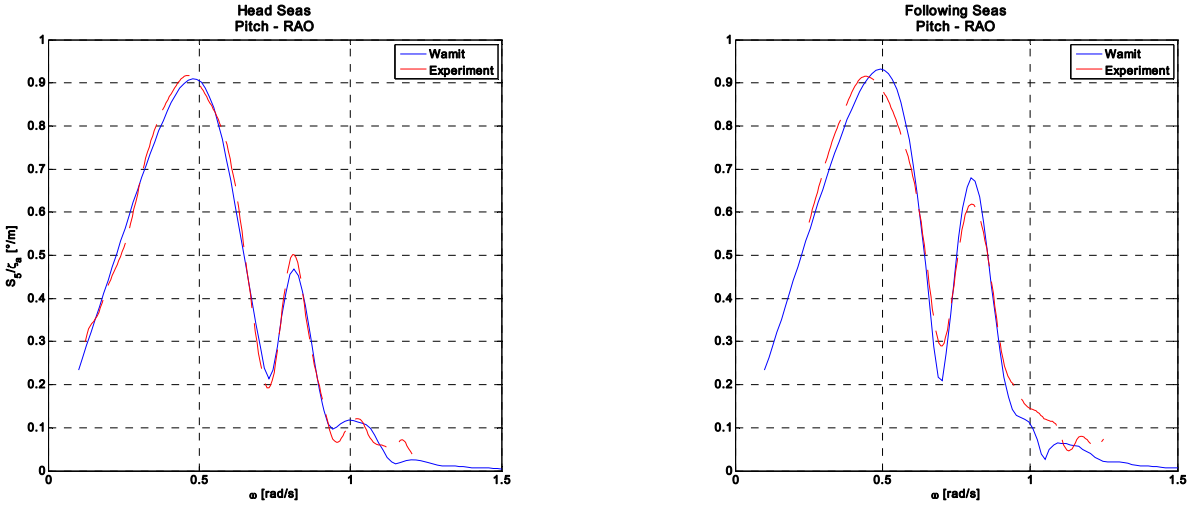

Fig. 8: Comparison of measured and calculated RAO for pitch motion

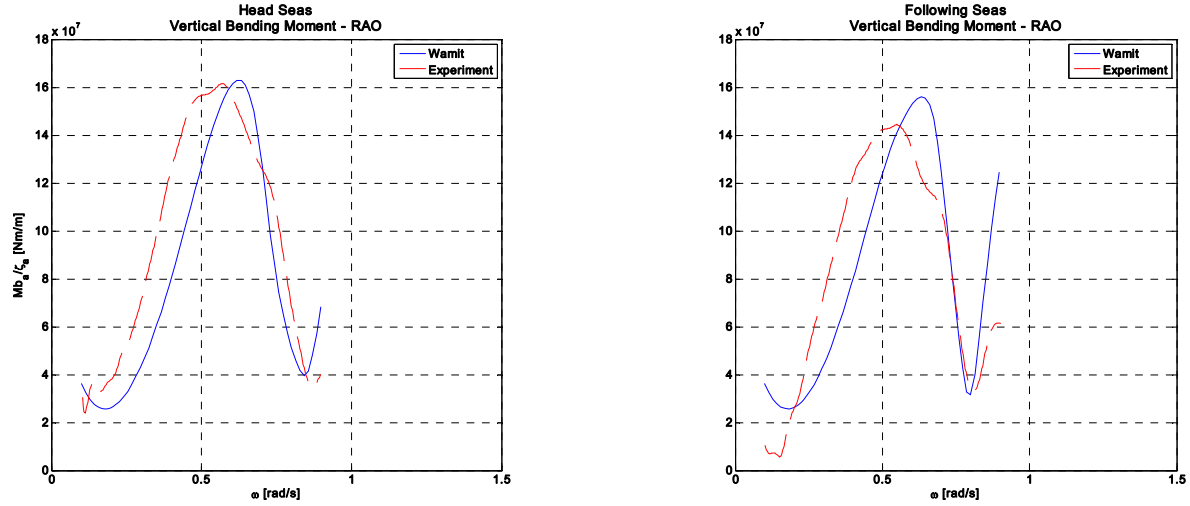

Fig. 9: Comparison of measured and calculated RAO for the bending moment

As illustrated in Fig. 7 and 8 the numerical results match the measured data in an excellent way regarding the Response Amplitude Operators (RAO) for the heave and pitch motion response. Both the curve progression and the location of the peaks regarding the amplitude as well as the phase are in good agreement. Also the comparison of the numerical and measured bending moments (Fig. 9) is satisfactory.

TIME DOMAIN RESULTS

To discuss the measured results in frequency- and time-domain they are compared to the design bending moments according to the IACS-Common Rules [2]. This design bending moment is calculated by empirical equations (Eq. 14 & 15) in combination with assumed design waves:

$$M_{WV,H} = 190 \cdot F_M \cdot f_p \cdot C \cdot L^2 \cdot B \cdot c_B \cdot 10^{-3} \qquad (14)$$

$$M_{WV,S} = 110 \cdot F_M \cdot f_p \cdot C \cdot L^2 \cdot B \cdot (c_B + 0{,}7) \cdot 10^{-3} \qquad (15)$$

depend on:

- F_M – distribution factor: $F_M = 1$ (midship)
- f_p – probability coefficient: $f_p = 1$
- C - wave parameter

$$C = \left[10.75 - \left(\frac{300 - L}{100} \right)^{1,5} \right]$$

- L – length of ship (= Lpp): L = 177.00 m
- B – moulded breadth of ship: B = 30.00 m
- c_B – total block coefficient:

$$c_B = \frac{\Delta}{1.025 \cdot L \cdot B \cdot T} = 0.818$$

- T – moulded draught: T = 11.80 m

With a wave parameter of C = 9.386, the design wave bending moments for the hogging and sagging condition, respectively, amount to

$M_{WV\text{-}hogging} = 1.37 \cdot 10^6$ kNm

$M_{WV\text{-}sagging} = 1.47 \cdot 10^6$ kNm

Note, that several additional parameters are to be considered before the final layout of the ship's hull is defined. At first a safety factor $\gamma_W = 1.2$ is introduced, leading to higher design wave bending moments:

$\gamma_W \cdot M_{WV\text{-}hogging} = 1.644 \cdot 10^6$ kNm

$\gamma_W \cdot M_{WV\text{-}sagging} = 1.764 \cdot 10^6$ kNm

To obtain the total design bending moment as basis for the hull dimensions, the still water bending moment has to be added too. As we are discussing dynamic effects only, this static contribution has not been considered.

Fig. 10 presents time domain results for the stationary condition (Froude number Fn = 0) at head seas. The blue graph represents the results for the target position at midship whereas the red line illustrates the results for the target position at the forward perpendicular. The first two diagrams show the surface elevation at the midship position and at the forward perpendicular, respectively. They illustrate that the NYW hits perfectly at the desired target position (crest height 19 m). As expected the highest loads occur during the impact of the freak wave. The heave motion displayed at the third diagram reaches a maximum of about +7 m and -6 m and the pitch angle illustrated at the 4th diagram amounts to nearly +10° and –7°, respectively. The measured bending moment at the 5th diagram exceeds with $1.53 \cdot 10^6$ kNm the design wave bending moment slightly but is within the limits considering the safety factor. Finally the bottom diagram shows the occurring longitudinal forces. With a maximum of up to $4.5 \cdot 10^4$ kN these forces can influence the loads at deck level or rather at keel level considerable, depending on the position of the neutral axis.

As shown in Fig. 11 the 'dynamic' neutral axis (based on the dynamic pressure forces) oscillates around 8.5 m above keel. Thus, it is located beneath the water line. As the point of action of the longitudinal force is identical to the position of the neutral axis, the longitudinal force ($4.5 \cdot 10^4$ kN) causes a counteracting moment compared to the vertical bending moment related to the waterline. With a lever arm of about 3.3 m the counteracting moment amounts to about $14.85 \cdot 10^4$ kNm which is 9.7 % of the vertical bending moment. That means that at waterline level the total bending moment due to the dynamic pressure forces is reduced by about 10 % through the counteracting moment caused by the longitudinal force. Depending on the hull geometry this value can raise significantly for other ship types. Furthermore the influence of the longitudinal force to the global stress raises with the distance from the neutral axis. Due to the large lever arms at deck and keel level, respectively, the stress levels in these areas due to the vertical bending moments are moderate whereas the longitudinal stresses are uniformly distributed and therefore do not change with increasing distance from the neutral axis.

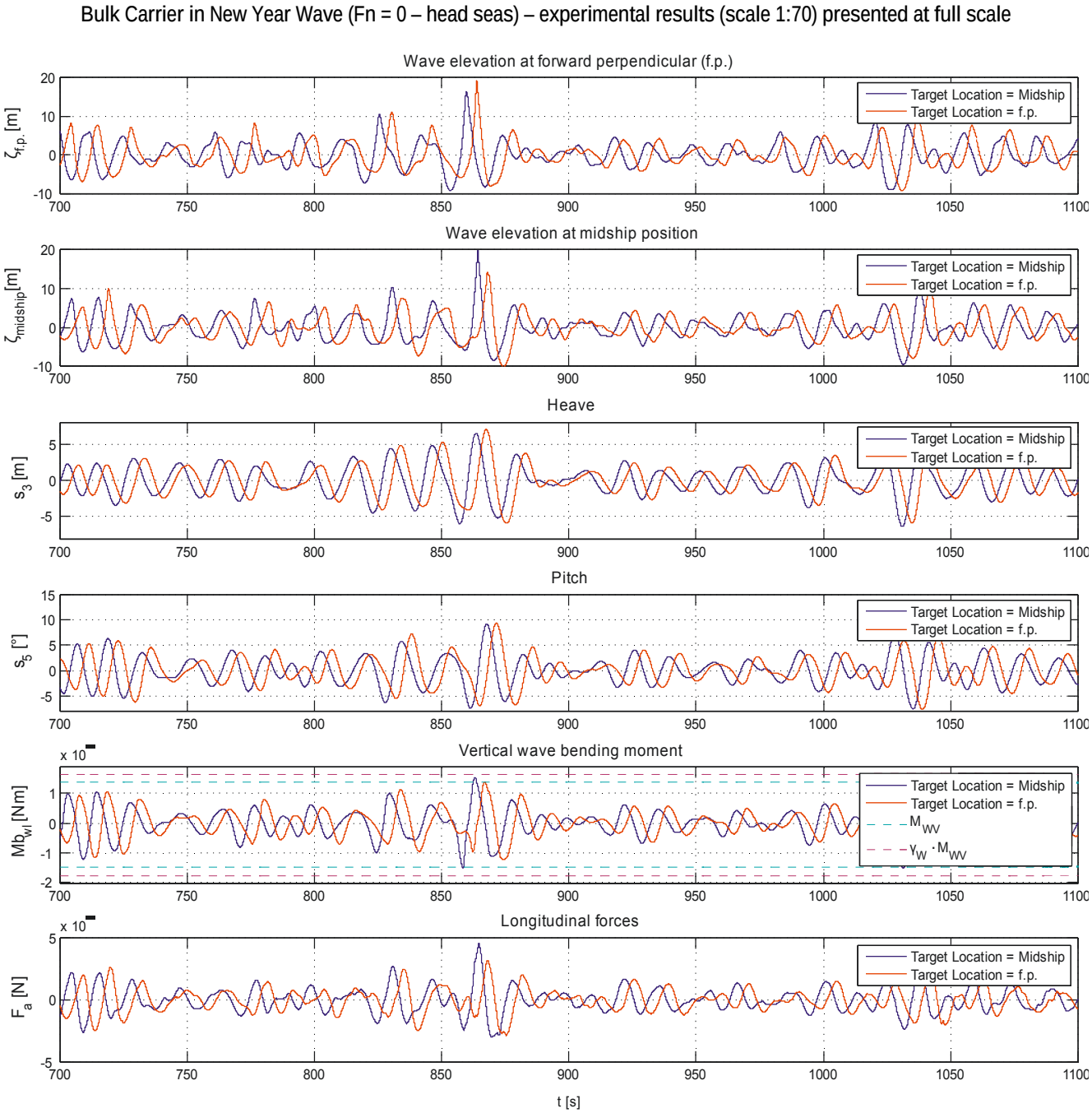

Fig. 10: Experimental results at Froude number Fn = 0 in head seas

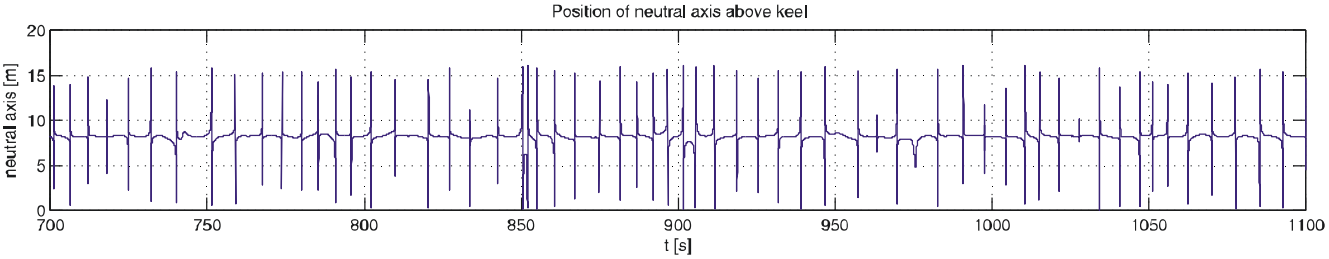

Fig. 11: Position of the neutral axis above keel

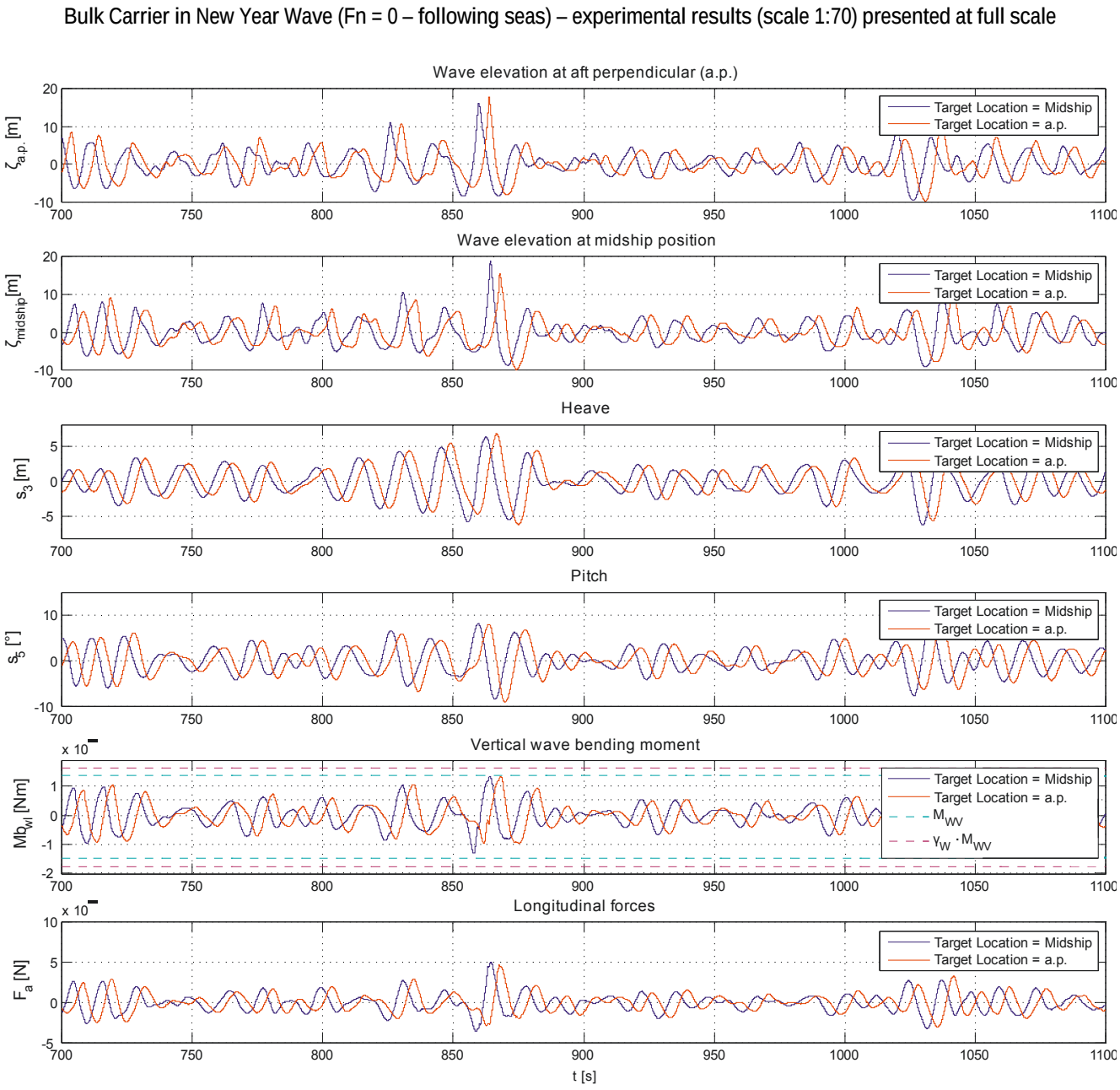

Fig.: 12: Experimental results at Fn = 0 in following seas

Fig. 12, 13 and 14 present similar diagrams at different conditions. Fig. 12 illustrates the stationary condition at following seas. Fig. 13 and 14 display the measured data at different cruising speeds for head seas (Fig. 13) and following seas (Fig. 14). Note that the results remain at the same level, but local differences can arise due to different encounter frequencies due to different cruising speed. It is remarkable that the design wave bending moment is already exceeded at about 770 seconds before the moment of the impact of the NYW although the waves are considerable smaller at this time (Fig. 13). Apparently in addition to wave height the sequence and encounter period of the occurring waves play a major role. Note that this applies especially to forward speed at head seas, because of the high impact velocity and encounter frequency.

Fig. 15 presents a photo series of the NYW-impact at target position forward perpendicular. The impact is extremely hard with the wave crest several meters above the bow. The delayed pitch motion of the bulk carrier causes huge amounts of green water on deck.

Bulk Carrier in New Year Wave (Fn = 0.15 – head seas) – experimental results (scale 1:70) presented at full scale

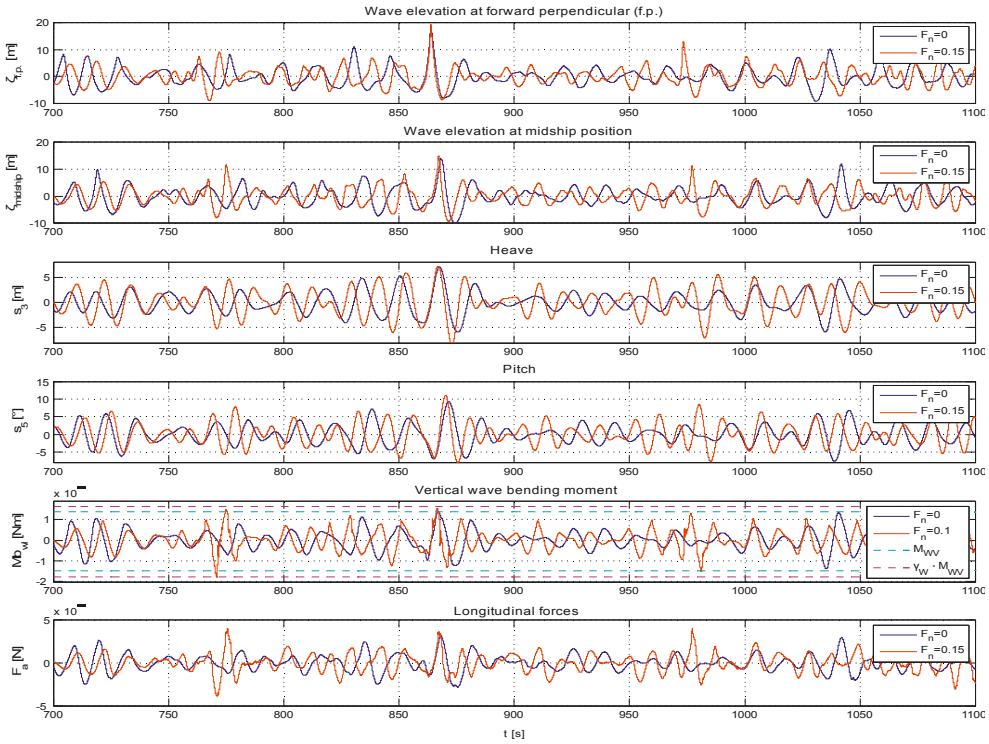

Fig. 13: Experimental results at Fn = 0.15 in head seas

Bulk Carrier in New Year Wave (Fn = 0.05 – following seas) – experimental results (scale 1:70) presented at full scale

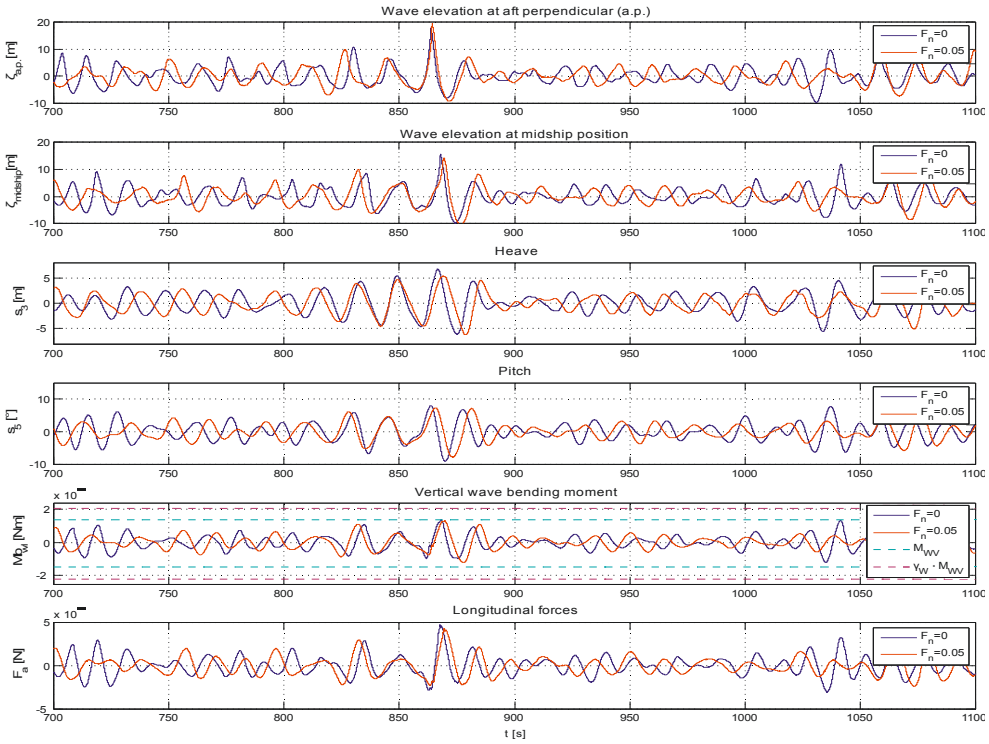

Fig. 14: Experimental results at Fn = 0.05 in following seas

CONCLUSIONS AND OUTLOOK

This paper presents a comprehensive study of the vertical bending moments of a bulk carrier due to rogue wave impact comparing numerical simulations and seakeeping model tests. A freak wave sequence registered in the North Sea has been generated at model scale using nonlinear methods. All model tests are performed with a segmented bulk carrier for measuring the vertical midship bending moment by three force transducers arranged at different vertical positions.

It is shown that the neutral axis is below the waterline level, with the consequence, that the associated longitudinal forces generate a counteracting moment.

The frequency-domain results of the numerical program system WAMIT are presented in comparison to model test data. The overall agreements is convincing although peak values and frequencies are slightly deviating regarding the bending moments.

In conclusion frequency-domain standard procedures for evaluating maximum bending moments turn out to be sufficient. However, time-domain investigations reveal specific wave/structure interaction effects (i.e. local impacts, green water). In numerical simulations as well as in seakeeping model tests we can state that even freak wave loads are covered by IACS-rules.

Fig. 15: Impact of the New Year Wave

ACKNOWLEDGEMENTS

This work has been developed in the scope of the project “HANDLING WAVES”, which is funded by the European Commission, under the contract TST5-CT-2006-031489. We highly acknowledge the support of this research project.

REFERENCES

[1] Clauss, G., Kauffeldt, A., Jacobsen, K., *Longitudinal Forces and Bending Moments of a FPSO*, Proceedings of 26th International Conference on Offshore Mechanics and Arctic Engineering (OMAE 2007), paper nr.: 29091, San Diego, USA, 2007

[2] Germanischer Lloyd, *IACS Common Structural Rules for Bulk Carriers,* Hamburg, Germany, 2008

[3] Kühnlein, W.L., Clauss, G.F., Hennig, J., *Tailor Made Freak Waves within Irregular Seas,* Proceedings of 21st International Conference on Offshore Mechanics and Arctic Engineering (OMAE’02), paper nr.: 28524, Oslo, Norway, 2002

[4] Clauss, G. F., Schmittner, C. E., *Experimental Optimization of Extreme Wave Sequences for the Deterministic Analysis of Wave/Structure Interaction*, Proceedings of 24th International Conference on Offshore Mechanics and Arctic Engineering (OMAE 2005), paper nr.: 67049, Halkidiki, Greece, 2005

[5] Clauss, G.F., Schmittner, C., Hennig, J., Guedes Soares, C., Fonseca, N., Pascoal, R., 2004, *Bending Moments on a FPSO in Rogue Waves*, Proceedings of 23rd International Conference on Offshore Mechanics and Arctic Engineering (OMAE 2004), paper nr.: 51504, Vancouver, Canada, 20-25 June, 2004

[6] Clauss, G.F., *The Taming of the Shrew – Tailoring Freak Wave Sequences for Seakeeping Tests*, 29. Georg-Weinblum-Lecturer, SNAME, David Taylor Model Basin, Washington, USA, June 07. 2007

[7] Clauss, G.F., Kühnlein, W.L., *Nonlinear Transient Wave Excitation as a new Tool in Model Testing*, International Conference on Offshore Mechanics and Arctic Engineering (OMAE 1996), paper nr.: OMAE1996-552, Florence, Italy, 16-20 June, 1996

[8] Haver, S. and Karunakaran, D., *Probabilistic Description of Crest Heights of Ocean Waves*, Proceedings 5th International Workshop on Wave Hindcasting and Forecasting, Melbourne, Florida, USA, 1998

[9] Department of Ocean Engineering, MIT, WAMIT, *WAMIT 5.2 – A Radiation-Diffraction Panel Program for Wave-Body Interactions*, User guide, 1994

[10] Bingham, H.B., *Simulating ship motions in the time domain*, PhD thesis, Massachusetts Institute of Technology (MIT), Cambridge, USA, 1994

[11] Cummins, W.F., *The impulse response function and ship motions*, Schiffstechnik, Band 9 (Heft 47):101-109, Germany, June 1962

[12] Bronstein, I.N., Semendjajew, K.A. and Musiol, G., *Taschenbuch der Mathematik*, G. Grosche & V. Ziegler, 1. Edition, 1993

[13] Newman, J.N., *Wave effects on deformable bodies*, Applied Ocean Research, 16:47-59, 1994

[14] Clauss, G., Stutz, K., Schmittner, C., *Rogue wave impact on offshore structures*, Proceedings of International Offshore Technology Conference (OTC), paper nr.: 161810, Houston, USA, 2004